Carbohydrate Polymers 272 (2021) 118477

Contents lists available at ScienceDirect

Carbohydrate Polymers

journal homepage: www.elsevier.com/locate/carbpol

Bioactive pectic polysaccharides from bay tree pruning waste: Sequential subcritical water extraction and application in active food packaging

E. Rincón [a,b], E. Espinosa [b], M.T. García-Domínguez [c], A.M. Balu [a], F. Vilaplana [d], L. Serrano [b], A. Jiménez-Quero [d,*]

[a] Departamento de Química Orgánica, Universidad de Córdoba, Campus de Rabanales, Edificio Marie-Curie (C-3), CTRA. IV-A, Km 396, E-14014 Córdoba, Spain
[b] Departamento de Química Inorgánica e Ingeniería Química, Universidad de Córdoba, Campus de Rabanales, Edificio Marie-Curie (C-3), CTRA. IV-A, Km 396, E-14014 Córdoba, Spain
[c] Departamento de Ingeniería Química, Química Física y Ciencia de los Materiales, Universidad de Huelva, Campus "El Carmen", Av. De las Fuerzas Armadas. S/N, 21007 Huelva, Spain
[d] Division of Glycoscience, Department of Chemistry, School of Engineering Sciences in Chemistry, Biotechnology and Health, KTH Royal Institute of Technology, Alba Nova University Centre, Roslagstullsbacken 21, 114 21, Stockholm, Sweden

ARTICLE INFO

Keywords:
Laurel
Circular biorefinery
Green extraction method
Antioxidant pectins
Food packaging films

ABSTRACT

The potential isolation of bio-active polysaccharides from bay tree pruning waste was studied using sequential subcritical water extraction using different time-temperature combinations. The extracted polysaccharides were highly enriched in pectins while preserving their high molecular mass (10–100 kDa), presenting ideal properties for its application as additive in food packaging. Pectin-enriched chitosan films were prepared, improving the optical properties (≥95% UV-light barrier capacity), antioxidant capacity (>95% radical scavenging activity) and water vapor permeability (≤14 $g \cdot Pa^{-1} \cdot s^{-1} \cdot m^{-1} \cdot 10^{-7}$) in comparison with neat chitosan-based films. Furthermore, the antimicrobial activity of chitosan was maintained in the hybrid films. Addition of 10% of pectins improved mechanical properties, increasing the Young's modulus 12%, and the stress resistance in 51%. The application of pectin-rich fractions from bay tree pruning waste as an additive in active food packaging applications, with triple action as antioxidant, barrier, and antimicrobial has been demonstrated.

1. Introduction

Due to the environmental considerations related to sustainable development addressed in recent years, a new trend of waste utilization has emerged. In particular, it is intended to use forest, agricultural and agri-food waste as source of new products capable of replacing those derived from petroleum. The main fractions of plant cell wall of these raw materials can be separated and purified for subsequent application in the so-called biorefineries of lignocellulosic materials (Ruiz et al., 2013).

Bay tree (*Laurus nobilis* L.), an abundant softwood in the Mediterranean, contains essential oils where its potential of application has been based until now (Rincón, Balu, Luque, & Serrano, 2019). However, bay tree is one of the most harvested crops of medicinal and aromatic plants around the world. According to Food and Agriculture Organization of the United Nations (FAO), the world production of spices, including bay tree, dill seed, fenugreek seed, saffron, thyme and turmeric, in 2019 was 2.7 million tons (FAO, 2019). Therefore, a large amount of residue is generated that can be used in different applications. The mixture of different plant tissues (leaves, stems, branches, and trunk) in the waste stream will impact the composition of the extracted polysaccharides, nevertheless, the valorization of all biomass by-products supposes a more sustainable approach for future biorefinery.

The main polysaccharides of the plant cell wall are cellulose and hemicellulose, together with lignin forming the mayor supramolecular structure of lignocellulose materials. Often pectins are forgotten in this structural equation. However, pectic polysaccharides can represent about 30% of the primary cell wall being located between cellulose microfilaments, which together with its complex structure makes its extraction from the cell wall difficult (Pasandide, Khodaiyan, Mousavi, & Hosseini, 2017; Rumpunen, Thomas, Badilas, & Thibault, 2002). Pectins are mainly composed by D-galacturonic acid and its methyl ester, followed by D-galactose, L-arabinose, and L-rhamnose (Marić et al., 2018). The concentration and proportion of the different

* Corresponding author.
E-mail address: amparojq@kth.se (A. Jiménez-Quero).

https://doi.org/10.1016/j.carbpol.2021.118477
Received 23 March 2021; Received in revised form 27 June 2021; Accepted 20 July 2021
Available online 24 July 2021
0144-8617/© 2021 The Authors. Published by Elsevier Ltd. This is an open access article under the CC BY license (http://creativecommons.org/licenses/by/4.0/).

monosaccharides in pectins will be influenced by the plant tissue and the age. Pectins are essential polysaccharides in the development of plant, notably in the cambial tissue, active growing tissue in wood plants (Coetzee, Schols, & Wolfaardt, 2011). In recent years, pectins have attracted increasing interest as a functional ingredient with great potential in areas such as cosmetics, food, pharmaceuticals, personal care products and active food packaging films (Marić et al., 2018; Maxwell, Belshaw, Waldron, & Morris, 2012).

Pectins functional properties are directly related to their structure, largely impacted by the extraction method (Chen et al., 2021). Traditionally, pectins are extracted from food processing by-products using severe acid extraction conditions at very low pH. In addition, these methods require high solid to liquid ratio and large solvent volumes. As result, the environmental impact is notably high, including extensive use of energy and water (Mao et al., 2019). More innovative pectin extraction technologies include ultrasound assisted-extraction, microwave assisted-extraction, high pressure processing (HPP), enzyme assisted-extraction, and subcritical water extraction. Subcritical water extraction (SWE) emerges as sustainable method in comparison with the conventional ones, allowing the isolation of polysaccharides while preserving their functionality and molecular mass. Subcritical conditions modify the properties of water, including viscosity, diffusion, polarity, and density surface tension. In addition to being effective, this process has proven to be scalable to the pilot scale (Rudjito, Ruthes, Jiménez-Quero, & Vilaplana, 2019). In subcritical conditions, water is at sufficient pressure to maintain its liquid state between its boiling and critical point, while reducing its polarity as a solvent as the temperature increases. Subcritical water at temperatures below 150 °C, can extract simple phenolic compounds, whereas at higher temperatures it is capable of hydrolyzing polysaccharides (hemicellulose and cellulose) to produce simple sugars and sugars oligomers (Lachos-Perez et al., 2020). Moreover, if SWE is done sequentially (S-SWE) at a fixed time and increasing the extraction temperature, it is possible to separate the different components of the lignocellulosic biomass.

As mentioned above, the applications of pectins are varied and, specifically, films involving pectins have been proposed for active food packaging (Gao, He, Sun, He, & Zeng, 2019). Due to the intrinsic hydrophilicity of pectins, pectin films tend to adsorb moisture, decreasing their mechanical strength and barrier properties (Norcino, de Oliveira, Moreira, Marconcini, & Mattoso, 2018). Some authors have reported that the use of pectins for film application is not very suitable if good water vapor barrier properties are required due to their strong hydrophilic character (Azeredo et al., 2016). However, it has also been reported that pectins, rich in simple sugars, have a plasticizing effect on polysaccharide films increasing the tensile strength. If they are included in very large quantities, these sugars decrease the concentration of the polymer matrix which may weaken the films (Otoni et al., 2014). In this context, blending of pectins with other biopolymers is carried out to improve the structural integrity and barrier properties of the films obtained (Lazaridou & Biliaderis, 2020), and conferring new functionalities that pectin films alone lack, such as antimicrobial capacity. Chitosan is a bio-based, non-toxic, biodegradable, bio-functional, and biocompatible polysaccharide and has antimicrobial properties, giving it immense potential as packaging material (Li, Kennedy, Peng, Yie, & Xie, 2006; Mathew & Abraham, 2008). In addition, chitosan has excellent film-forming properties, enabling it to mitigate the difficulties of using pectins and other polysaccharides in food packaging. Moreover, chitosan has many hydroxyl and amine groups that can form hydrogen bonds with polysaccharides, thus conferring a good miscibility to the structure (Xu, Xia, Zheng, Yuan, & Sun, 2019). The use of chitosan for the formulation of pectin-additivated films could provide certain advantages such as reducing the water sensitivity of pectins, and thereby increasing the barrier properties (Ren, Yan, Zhou, Tong, & Su, 2017). Furthermore, as mentioned above, chitosan has antimicrobial character and therefore it is expected that chitosan-pectin blends will maintain these properties, favoring their application for active food packaging.

This work reports the extraction of polysaccharides by S-SWE from bay tree pruning waste (BTPW), enriched in pectic polymers. The optimal conditions of temperature and time were decided based on the extraction yield, the carbohydrate profile and the molar mass distribution. The extracted polysaccharides were applied as additive in chitosan-based films and their thermo-mechanical and bioactive properties were validated for food packaging applications.

2. Materials and methods

2.1. Materials

Bay tree pruning waste (BTPW) used in this study was kindly supplied by an independent farmer from Arjonilla (37°58′27″N–4°06′27″W), in the province of Jaén, Spain. BTPW consisted of a mixture of leaves, stems, branches, and trunk. Prior extractions and analyses, sample was ground, sieved (0.25–0.40 mm), and washed with plain water and hot air-dried at 55 °C to a moisture level below 10%. The raw material was then characterized according to standard methods (Technical Association of the Pulp and Paper Industry, TAPPI Standards, 2018): 30.84 ± 0.39% cellulose; 17.58 ± 0.39% hemicelluloses; 22.31 ± 1.12% lignin; 4.87 ± 0.43% ash; and 17.05 ± 0.94% alcohol extractable. The carbohydrate content of BTPW was 451.79 mg/g (2.04 mg/g fucose; 37.06 mg/g; 29.77 mg/g galactose; 236.68 mg/g glucose; 107.09 mg/g xylose; 7.37 mg/g mannose; 31.69 mg/g uronic acids) as reported in a previous investigation (Rincón et al., 2020).

Chitosan (high molecular weight 310,000–375,000 Da, >75% deacetylated chitin, poly(D-glucosamine) was purchased from Sigma-Aldrich (Spain). All other chemicals used in this study were of analytical grade and purchased from Sigma-Aldrich Inc. (Sweden), unless otherwise stated.

2.2. Sequential subcritical water extraction (S-SWE)

Sequential subcritical water extraction (S-SWE) of BTPW was performed using a laboratory accelerated solvent extraction Dionex™ ASE™ 350 (Thermo Fisher Scientific Inc., USA). A total of 5 g of BTPW was placed into an extraction cell sandwiched between ASE Extraction Cellulose Filters (Thermo Fisher Scientific Inc., USA). BTPW was then sequentially extracted using tap water (pH 7.3) for fixed times (5, 10, 15, and 20 min) at four increasing temperatures (100, 120, 140 and 160 °C). The extractor kept a solid to liquid ratio of 1:8 (w/v). After extraction, polysaccharides were purified by ethanol precipitation (ethanol:liquid ratio 3:1) standing at 4 °C during 24 h. Two fractions were obtained (Fig. 1a): liquors (L, liquid fraction before ethanol precipitation), and purified polysaccharides (P, carbohydrates obtained after ethanol precipitation). The fractions obtained during the extraction process (L and P) were freeze-dried (FreeZone 6, Labcombo, USA) before further analysis.

The severity factor R_0 for each SWE was calculated (Table S1) according to the Eq. (1) proposed by De Farias Silva and Bertucco (2018):

$$R_0 = e^{(T-Tr)/\omega_t} \quad (1)$$

where T is the holding temperature of the process (°C), Tr is the reference temperature (100 °C), t is the holding time of the extraction (min), and ω is a parameter representing a first-order approximation of the temperature dependence of the Arrhenius equation, generally assumed equal to 14.75.

2.3. Analytical methods

2.3.1. Yield determination

Cumulative extraction yield (%) was calculated gravimetrically based on the extracted dry matter present in the L-fraction for each S-

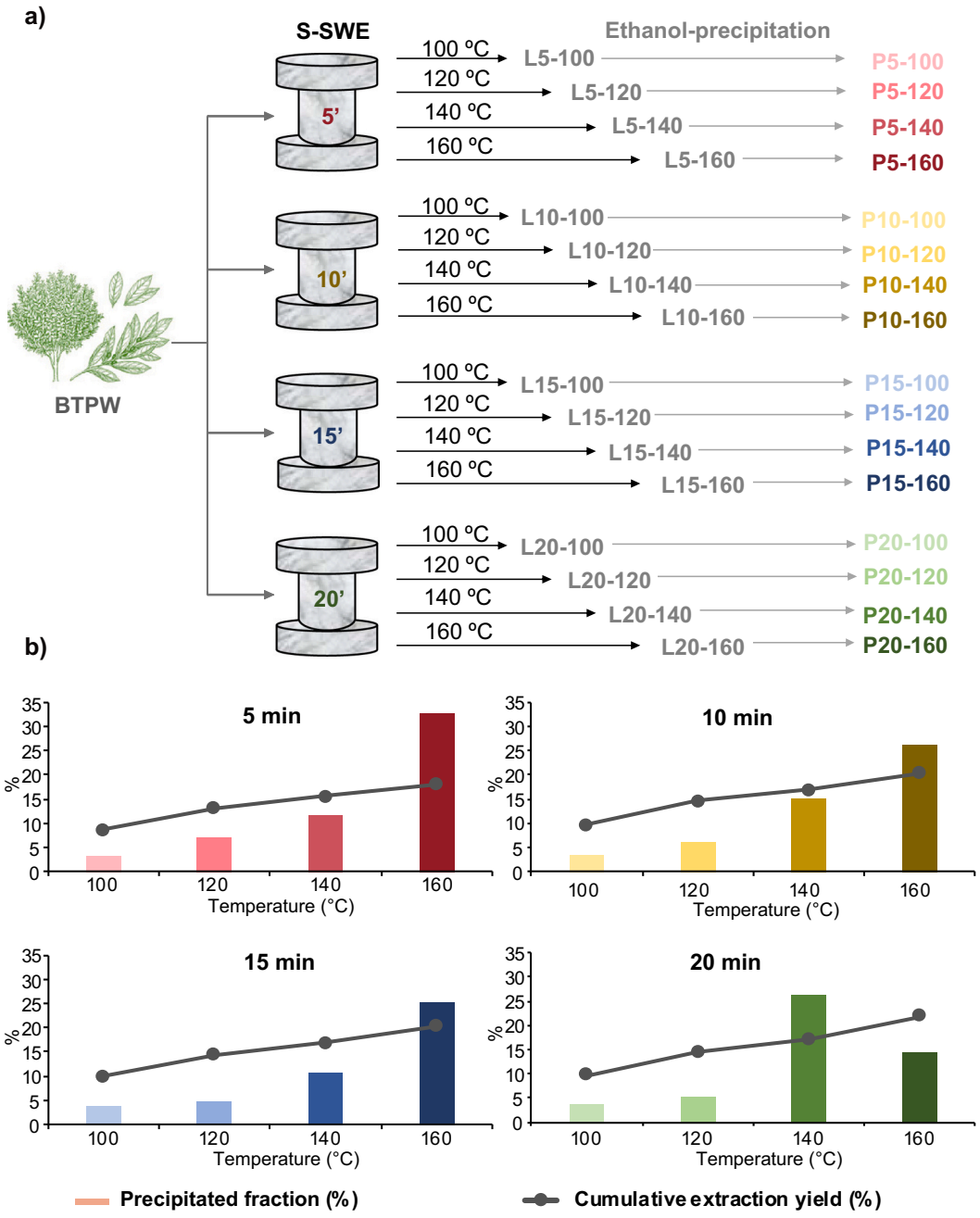

Fig. 1. a) Scheme of sequential subcritical water extraction (S-SWE) of bay tree pruning waste (BTPW) extracted fractions and b) cumulative extraction yield and polymeric precipitated fraction (%) of BTPW-S-SWE.

SWE phase relative to the initial dry-BTPW biomass. Similarly, polymeric precipitated fraction (%) was gravimetrically determined based on the dry precipitated P-fraction relative to the dry weight of each corresponding L-fraction.

2.3.2. *Molar mass distributions*

The molar mass distributions of the L and P fractions was determined by size exclusion chromatography (SEC) in a SECurity 1260, Polymer Standard Services (Germany) according to the method used by Ruthes, Martínez-Abad, Tan, Bulone, and Vilaplana (2017).

2.3.3. *Monosaccharide composition*

The monosaccharide composition in L and P fractions were analyzed and quantified by High-Performance Anion-Exchange Chromatography with Pulsed Amperometric Detection (HPAEC-PAD) on an IC3000 system (Dionex, USA) using a Dionex CarboPac PA1 column at 30 °C at a flow rate of 1 mL/min. Two different gradients were applied for the analysis of neutral sugars (fucose, arabinose, rhamnose, galactose, glucose, xylose and mannose) and uronic acids (galacturonic, glucuronic and 4-*O*-methyl-D-glucuronic acids) as reported by McKee et al. (2016).

Prior to analysis, samples were subjected to methanolysis followed by trifluoroacetic acid (TFA) hydrolysis (Requena et al., 2019).

2.3.4. *Phenolic acids*

The analysis of phenolic acids was conducted by (high-performance liquid chromatography (HPLC) in a ZORBAX StableBond C 18 column (Agilent Technologies, USA) fitted to a separation module (Waters 2695, USA) coupled to a photodiode array detector (Waters 2996, USA). A gradient method was performed with 2% acetic acid and methanol as eluents as reported by Menzel, González-Martínez, Chiralt, and

Vilaplana (2019). Samples were subjected to overnight saponification with NaOH solution at 2 M at 37 °C with stirring, before the analysis.

2.4. Chitosan-based films preparation

Films were prepared by solvent casting method with a grammage of 35 g m^{-2}. For the preparation of films, a 1% (w/v) chitosan solution (CH) in 1% (v/v) aqueous acetic acid solution was prepared. CH films (used as control film) were prepared by diluting the initial CH solution in aqueous acetic acid until 0.4% solid content at magnetic stirring for 24 h at 25 °C. The forming dispersion was cast in the center of levelled Petri dished and dried at room temperature (25–30 °C). On the other hand, CH films incorporating the selected P-fraction (P5-160) were prepared. For this, a 2% (w/v) P-fraction solution in 2% (v/v) aqueous acetic acid was prepared by mixing P and the aqueous acetic acid with magnetic stirring for 24 h at 60 °C. CH-based films containing P were prepared by mixing the 1% CH solution with 2% P solution to achieve final CH:P ratios of 90:10, 80:20, 70:30, and 60:40 (1.01%, 1.02%, 1.04%, and 1.08% (v/v) acid concentration in the final solutions, respectively, with pH values in the range of 2.10–2.20). Hybrid films were prepared as described above. The as-obtained films were labelled according to the CH:P ratio: 100% CH, 90:10 CH:P, 80:20 CH:P, 70:30 CH:P, and 60:40 CH:P. Before characterization, films were conditioned at 25 °C and 50% relative humidity for three days.

2.5. Characterization of the films

2.5.1. Fourier Transform Infrared Spectroscopy (FTIR)

CH, P, and films were characterized by attenuated total reflectance Fourier transform infrared spectroscopy (ATR-FTIR) in a Perkin-Elmer Spectrum Two collecting over 20 scans with a resolution of 4 cm^{-1} in a wavenumber range between 4000 and 400 cm^{-1}.

2.5.2. Thermogravimetric analysis (TGA)

The thermogravimetric analysis of the prepared films was carried out using a TA Instrument TGA Q50 thermogravimetric analyzer (Mettler-Toledo, Barcelona, Spain). The measurements of weight loss of the samples in relation to the temperature of thermal degradation were carried out between 50 and 800 °C at 10 °C/min under a N_2 flow (20 mL/min).

2.5.3. Physical properties: density and barrier properties against water vapor

Density of the prepared films was measured by weighing a square of 1 cm^2 of film sample of known thickness (determined with a micrometer Digital Micrometer IP65 0-1″, Digimatic, Mitutoyo, Neuss, Germany with a sensitivity of 0.001 mm). This determination was performed in triplicate.

Water vapor permeability (WVP) of prepared films was determined according to ASTM E96/E96M-10 (International, 2010). Briefly, WVP was measured as the change in weight of sealed plastic containers (containing desiccant material), whose lids were perforated with a 10 mm diameter circle where the film sample was placed, in an atmosphere of controlled temperature (25 °C) and RH (50%) for 24 h.

2.5.4. Mechanical properties

Mechanical properties evaluation was performed using a Universal Testing Machine, model LF Plus Lloyd Instrument AMETEK Measurement & Calibration Technologies Division (Largo, FL, USA). These tests included traction stress, Young's modulus, and strain according to ASTM D882 standard method (International, 2018). Before measurements, all the films were cut in strips (1.5 × 10 cm) and equilibrated at 25 °C and 50% relative humidity (RH) according to the standard method. Then they were fixed between the grips with an initial separation of 65 mm, and the crosshead speed was set at 10 mm/min and 1 kN load cell. Results were expressed as an average of eight samples for each film.

2.5.5. Optical properties

The transparency and UV-blocking capacity of the prepared films was determined by measuring the transmittance in the UV–VIS region (200–800 nm) in a Perkin Elmer UV/VIS spectrometer Lambda 25 (Waltham, Massachusetts). The thickness of each film sample was measured as described above and used to calculate transparency (Eq. (2)) and UV-light barrier capacity (Eq. (3)).

$$\text{Transparency } (\%) = \frac{log\%T_{660}}{x} \quad (2)$$

$$\text{UV} - \text{blocking capacity } (\%) = 100 - \left(\frac{\%T_{280}}{\%T_{660}}\right) \times 100 \quad (3)$$

where, $\%T_{660}$ and $\%T_{280}$ are the percent transmittance at 660 nm and 280 nm, respectively, and x is the film thickness (mm).

2.5.6. Radical scavenging activity by DPPH

The radical scavenging activity of the CH and P-fraction was determined by the 1,1-diphenyl-2-picrylhydrazyl (DPPH) assay according to the method of Brand-Williams, Cuvelier, and Berset (1995). Briefly, 100 μM methanolic $DPPH^{\bullet}$ solution was mixed with different volumes of aqueous sample solutions (1, 5, 10, 20, 40, 60, 80, 100 μL). The reaction mixtures were kept in the dark at room temperature for 30 min. The resulting absorbances were measured at 517 nm using a microplate reader (Clariostar Plus, BMG LABTECH, Germany). Ferulic acid and ascorbic acid were used as comparative control. The results were expressed as EC_{50}, which represents the concentration of antioxidant required to decrease the initial concentration of $DPPH^{\bullet}$ by 50%. In the case of film samples, the radical scavenging activity was calculated from the percentage of $DPPH^{\bullet}$ content remained in the solution after in three addition cycles of the oxidative radical.

2.5.7. Antibacterial properties

Minimum inhibitory concentration (MIC) of pure CH was determined against three test organisms: typical food pathogen bacteria were used for the antimicrobial testing including a Gram-negative representative, *Escherichia coli* (CCUG 10979), and two Gram-positive representatives, *Listeria innocua* (CCUG 15529) and *Bacillus cereus* (CCUG 7414) in serial dilution (10 to 2.5 mg/mL) adapting the method reported by Casado Muñoz, Benomar, Lerma, Gálvez, and Abriouel (2014). The assay was adapted to microplate volumes (final volume 0.2 mL), CH dilutions were transferred into the well microplate together with LB medium (Lysogeny Broth) containing the microorganisms (previously adjusted to a concentration of 10^5 cells/mL). LB medium alone was used as negative control and LB with the bacteria as positive control. The microplate was then incubated at 37 °C for 24 h and the absorbance was read at 517 nm using a microplate reader (Clariostar Plus, BMG LABTECH, Germany) determining signs of bacteria growth or turbidity after the period of incubation. The lowest concentration of CH that inhibited the growth of bacteria was considered as the MIC.

The antimicrobial activity of film samples was assessed against *E. coli*, *B. cereus*, and L. *innocua* by the agar diffusion method. Microbial strains were inoculated in LB medium at an appropriate temperature for 12 h. Young-type strains (50 μL from growth at 37 °C of the different bacteria) were coated on solidified nutrient agar plates. Film samples were cut into 9 mm diameter circular discs and placed on the nutrient agar plate's surface. Inoculated plates were incubated at 37 °C for 24 h. The antimicrobial activity of the test microorganisms was evaluated by measuring the antibacterial inhibition zone.

3. Results and discussion

3.1. Mass balances

Cumulative extraction yield represented the sum of dry weight of the

extracted liquid (L) fractions after S-SWE, together with the polymeric precipitated (P) fractions from the different L fractions by ethanol precipitation are shown in Fig. 1b. The trend for the cumulative extraction yield was very similar in the different set up times for the experiments with final yields between 18.06% for 5 min S-SWE and 21.76% for S-SWE cycles of 20 min (Table S1). This low increase on yield over extraction time could be due to the saturation of the aqueous phase in term of solubilized compounds as reported previously (Rudjito et al., 2019). Moreover, the non-pretreated plant tissues of BTPW with high content in low molecular mass extractives allowed yields around 20%, lower than in a similar study using hot water conditions on spruce bark, another softwood biomass, with a total yield obtained of around 40% (Le Normand, Edlund, Holmbom, & Ek, 2012). Nonetheless, in this study the initial bark tissue was pure, after previous acetone extraction. Moreover, the authors performed 3 cycles of 20 min for each subsequence temperature, so a total of 180 min, while in the present study a total extraction time of 20 min (4 times at 5 min) already released around 20% of the dry weight of the BTPW. In another study using root bark, stem bark and leaves of *Terminalia macroptera* for hot water extraction of pectins, 2.5% from the total DW was obtained (Zou et al., 2014). This was a relatively lower yield compared with 8.7% obtained in the present study using similar conditions (5 min 100 °C) for extraction of BTPW. This indicated that S-SWE is a desirable method for the extraction of polysaccharides from BTPW, with the possibility to obtain mixed carbohydrate fraction in a soluble state.

This same behavior could be observed for the polymeric precipitated fractions. When the temperature was increased during the same S-SWE time the total precipitated weight was considerably increased. For example, at 5 min the polymeric precipitated fraction increased from 3.10 to 32.68% (Table S1) when temperature was increased from 100 to 160 °C. In fact, the maximum precipitated fraction was achieved under these conditions. As previously mentioned, this trend is to be expected since the use of S-SWE leads to the extraction of extractives and more soluble carbohydrates at temperatures below 150 °C, while above 150 °C polysaccharides are obtained (Lachos-Perez et al., 2020). SWE of carbohydrate polymers combines a mix of procedures: as the polymers are solubilized and detached from the biomass network, they can undergo hydrolysis simultaneously at high temperatures, causing a diffusion out of the lignocellulosic material and dissolution into the aqueous solvent. These factors impact the mass transfer at subcritical condition which allow to tune the extraction yield by controlling both temperature and time. Consequently, in the case of longer sequential cycles of SWE, as 20 min, the trend in the extraction changed since the maximum polysaccharides precipitated was obtained at 140 °C (26.20%) instead at 160 °C (14.37%). This fact has been previously reported by other authors who carried out the fractionation of red wine grape pomace using S-SWE and observed a decrease of polymeric carbohydrate due to depolymerization under hasher conditions (Pedras et al., 2020).

3.2. Extractability and characteristics of carbohydrate populations

3.2.1. Carbohydrates and phenolic compounds

The carbohydrate profiles as well as the phenolic compounds found in the liquor (L) and precipitated (P) fractions are displayed in Fig. S1 and Fig. 2a, respectively. Regarding the L fractions, the amount of total carbohydrates augmented when temperature increased for the same fixed time. As an example, when the S-SWE was carried out in 5 min cycles, the total carbohydrates extracted were 217.88, 230.27, 287.99 and 618.88 mg carbohydrates/g of BTPW, in the increasing temperatures from 100 to 160 °C, respectively (Table S2). The carbohydrate composition showed that L5-160, L10-160, and L15-160 were mainly composed of pectins and secondarily by hemicelluloses, where galacturonic acid, arabinose, rhamnose and galactose where the main monosaccharides in the extracts. Therefore, the change in temperature from 140 to 160 °C resulted in a major change in the composition of L fraction with an increased extractability of pectic polymers. Other authors reported similar results due to the increase in the extraction temperature for citrus peel (Chen et al., 2021; Zhang et al., 2018) and watermelon rind (Petkowicz, Vriesmann, & Williams, 2017). The large amount of glucose present in all the samples was attributed to starch, which is more extractable and can be solubilized at shorter and lower temperature conditions as previously reported (Rudjito et al., 2019). Increasing amount of arabinose might come from different kinds of polysaccharides in the biomass, such as highly branched arabinans and arabinogalactans, hydrolyzed at higher temperature which explain the decrease in P-fraction after ethanol precipitation (Wandee, Uttapap, & Mischnick, 2019).

These facts were evident in all the extractions carried out at 5, 10 and, 15 min. However, in the case of S-SWE at 20 min, the highest amount of carbohydrate was obtained at 120 °C. This is because longer cycles allow an earlier polysaccharides extraction due to the greater severity of the treatment, yielding a lower carbohydrate content available for extraction in subsequent cycles.

The phenolic compounds in these L fractions increased, in general, as the extraction temperature increased. These data were closely related to the severity factors of the extraction conditions, cleaving the ester bound of the phenolic decorations on the carbohydrates. As previously reported, the more severe the extraction, the higher was the amount of ferulic acid obtained from BTPW (Rincón et al., 2020).

The characterization of the P-fraction obtained after ethanol precipitation (Fig. 2a and b) were enriched in carbohydrates with respect to their corresponding liquor fraction. At short S-SWE times (5 and 10 min), the highest amount of carbohydrates was obtained at the highest temperature (676.73 and 873.72 mg/g for P5-160 and P10-160, respectively, Table S3). At longer S-SWE times (15 and 20 min), the highest amount of carbohydrates was obtained at 140 °C. As previously mentioned, longer extraction time cycles allow to use lower extraction temperatures.

Pectins are very complex polysaccharide structures with a rich variety of glycosidic linkages, where galacturonic acid and rhamnose are usually found in the backbone, with diverse side chains of arabinose, galactose, and glucuronic acid. All these monosaccharides were present in BTPW as reported previously (Rincón et al., 2020). Enriched fractions on galacturonic acid were seen after precipitation, which allowed us to conclude the extraction of polymeric pectins during the S-SWE after reaching 140 °C. The most remarkable result was in the P5-160 sample with a high amount of galacturonic acid (GalA, 36.24% of carbohydrates in the fraction, Table S3), and the greatest yield of precipitated polysaccharides from the liquid extract (32.68%, Fig. 1), confirming that polymeric pectins were with this S-SWE conditions. Regarding galactose and mannose, the fact that there was more galactose than mannose suggested that galactose probably came from galactans or arabinogalactan (AG) pectins. These results suggested that pectins, containing uronic acids, are easily extractable by SWE, especially at short times as reported in previous investigations (Ruthes et al., 2020).

The phenolic acids profiles in P-fractions seemed to indicate that S-SWE maintained the polymeric structure of pectins and, more interesting, preserved their functional phenolic acids attached (Ruthes et al., 2017). Interestingly, P5-160 showed the highest amount of phenolic acids that precipitated together with the carbohydrates, mainly pectins (Table S3). This shorter time of extraction seemed to favor the solubilization of polysaccharides preserving the ester bound phenolics as previously reported for hemicelluloses from cereal by-products (Rudjito et al., 2019). The extraction of phenolic group linked to pectins has been reported previously, identifying mostly ferulic acid in sugar beet pectins (Rombouts & Thibault, 1986).

3.2.2. Molar mass distributions

The molar mass distributions of the different S-SWE fractions were studied by size exclusion chromatography (SEC) of L-fractions (Fig. S1c) and P-fractions (Fig. 2c). In general, the polymodal distributions are due to the mix of different polysaccharide components in the tissues from

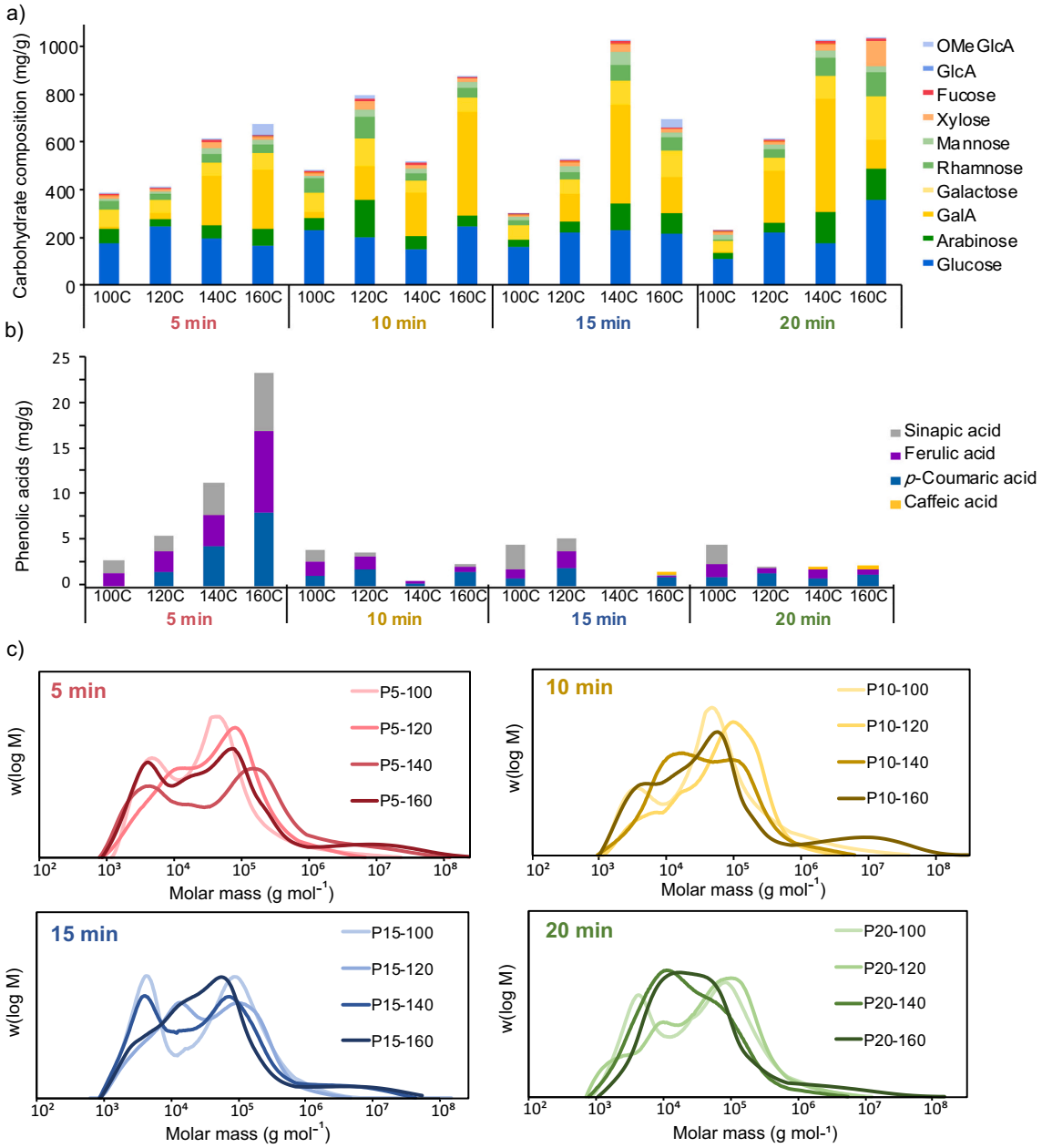

Fig. 2. a) Carbohydrate composition, b) phenolic acids content and c) molecular mass distribution of the pectic (P) fractions from bay tree pruning waste (BTPW).

BTPW. The P-fractions presented a range between 10^3 and 10^6 g/mol after ethanol purification (Fig. 2c) while in the L-fractions (Fig. S1) smaller molar mass populations were shown. The extraction at higher temperature resulted in the presence of a bigger molar mass population around 10^7 g/mol, probably assigned to aggregated pectin structures or residual starch. Using shorter extraction times, 5 and 10 min cycles the population between 10^4 and 10^5 g/mol were mostly preserved, possibly corresponding with pectins and hemicellulose extracted as reported before (Rincón et al., 2020). This result indicated that short extraction cycles, but high extraction temperatures result in pectins with predominant high molecular mass in the sample (Yang, Mu, & Ma, 2018).

The results obtained suggested that S-SWE is a suitable methodology to extract polymeric carbohydrate from BTPW while preserving their phenolic substitutions and structure. Based on the desired application, extraction of high molecular mass and high phenolic content pectins is required for applications as structural and active additive in food packaging. Therefore, the conditions of S-SWE 5 min at 160 °C were selected for further development.

3.3. BTPW-pectins in CH-based films

Jin et al. (2019) reported in literature the potential of high molecular mass polysaccharides in films by improving barrier and mechanical properties. In the present study, P5-160 fraction was chosen because of the high polymeric composition and the interesting phenolic acids profile, which could improve the mechanical strength of the films as well as provide antioxidant properties. In this sense, CH-based films were prepared with different concentrations of P5-160 (from 0 to 40 wt%, Fig. 3a).

The FTIR spectra of CH, P5-160 fraction and their hybrid films are shown in Fig. 3b and c. The broad peak between 3000 and 3500 cm^{-1} was due to the O—H stretching of the carbohydrate in CH and P5-160 samples, and the N—H stretching specifically of CH only. In the same way, the absorption bands from 1300 to 800 cm^{-1} are referred to the

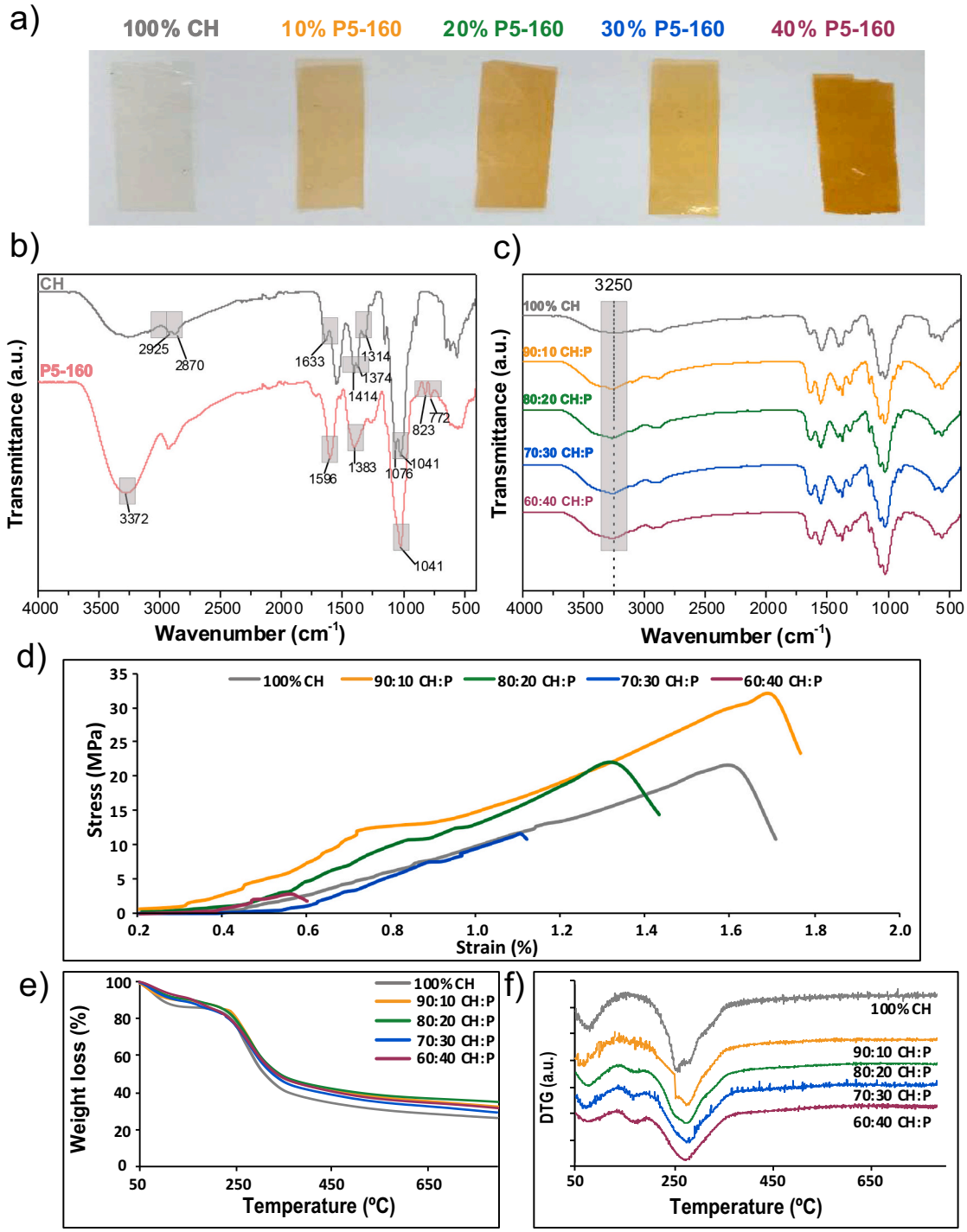

Fig. 3. a) Visual transparency of chitosan:pectins (CH:P) hybrid films, b) Fourier transform infrared spectroscopy (FTIR) spectra of CH and P5-160 fraction, c) FTIR spectra, d) strain-stress curves, e) Thermogravimetric analysis (TGA) and f) Derivative thermogravimetry (DTG) curves of CH:P hybrid films.

fingerprint region of carbohydrates (Costa et al., 2015; Yang et al., 2018). Specifically for CH, the diagnostic bands include 1633, 1590, and 1314 cm^{-1} were assigned to amide I, $–NH_2$ bending, and C—N stretching vibrations, respectively (X. Zhang et al., 2020). In the case of the P5-160 sample the peak at 1596 cm^{-1} was assigned to C═O stretching of methyl esters and carboxylic acid in pectin. Lastly, the peaks at 823 cm^{-1} and 772 cm^{-1} indicate the degree of methyl esterification. This region of pectins fingerprint is unique for the compound and is usually difficult to interpret (Santos et al., 2020).

In the case of hybrid film samples, the O—H stretching band shift to lower wavenumbers, from 3372 to 3250 cm^{-1}, was an indicative that interactions through hydrogen bonding between P5-160 carbohydrates and CH became stronger due to the blending process (Norcino et al., 2018). Moreover, it is worth mentioning the higher intensity of the peak at 1655 cm^{-1}, characteristic of amide I, as the amount of pectins in the films increases.

The thermogravimetric analysis (TGA) curves for CH:P hybrid films in shown in Fig. 3e. In all cases, the typical TGA curves for weight loss as a function of temperature can be observed. Thus, both the 100% CH films and those including P5-160 fraction started to degrade around 226 °C. At 100 °C, two thermal degradation events were observed (Fig. 3f). The first thermal event was a weight loss in the range of

50–100 °C, which is due to the evaporation of water from the sample, while the second event was observed around 230 °C attributed to the decomposition process of the film. In addition to these two events, in the case of the CH:P hybrid films, a third thermal degradation event was observed around 160–200 °C, which became more pronounced as the amount of P5-160 fraction in the film increased. This event is attributed to the depolymerization of pectin chains (Maciel, Yoshida, & Franco, 2015). As in the case of the blank film, the decomposition process of the samples started at about 250 °C. Thus, the higher the P-fraction in the film, the lower the maximum degradation of the material. Younis, Abdellatif, Ye, and Zhao (2020) reported that the interaction between the amino groups of CH and the carboxyl groups of P-fraction protects CH molecules against the thermal-induced deamination.

3.4. Physical and mechanical properties of pectin CH-based films

The density values obtained for the prepared films are displayed in Table 1. As shown, the density of the films slightly increased with the inclusion of P5-160 up to 20% (density values of 0.91, 1.03 and 1.09 g/cm^3 for 100% CH, 90:10 CH:P, and 80:20 CH:P, respectively). This is because the interactions between the polymer chains in the CH and the added BTPW fraction can be strongly established increasing the cohesion of the polymer network forces (Xu, Xia, Yuan, & Sun, 2019; Zhang, Wei, et al., 2020). Thus, hydrogen bonding complexes are formed since CH acts as an ionic crosslinking agent with P5-160. Whether this crosslinking is effective depends mainly on four factors: charge density, distribution of electric charges in each polymer chain, pH and ionic strength (Norcino et al., 2018). These ionic bonds influence both the water adsorption and mechanical properties of the films. When the amount of P5-160 in the films was greater than 20%, the density started to slightly decrease until it reached 0.84 g/cm^3 at of 40%. This indicates that higher pectic content does not improve the network assembly and the interactions between polysaccharide chains, resulting in a lower densification of the structure.

Water vapor permeability (WVP), shown in Table 1, measures the mobility of water molecules through the film. When films are to be applied to food products, this property indicates the exchange of moisture through the packaging film and the atmosphere. It is a dependent factor on several parameters such as surface hydrophilicity, thickness, and matrix microstructure (Younis et al., 2020). Addition of pectin in the film matrix has proven to improve the water resistance by increasing cross-linking between polymer chains (Almasi, Azizi, & Amjadi, 2020). Thus, the hydrophobic/hydrophilic balance for P5-160 fraction plays a key role since hydrophobicity is increased and fraction of low molecular mass is high (Table S3).

The blank film (100% CH) showed a WVTR and WVP values of 53.21 g·m^{-2}·h^{-1} and 17.76 g·Pa^{-1}·s^{-1}·m^{-1}·10^{-7}, respectively, in accordance with (Xu, Kim, Hanna, & Nag, 2005). The increase in the P5-160 fraction in the CH matrix resulted in a decrease in WVP. Thus, the film containing 10% pectins presented a WVP value of 14.53 g·Pa^{-1}·s^{-1}·m^{-1}·10^{-7} (Table 1), decreasing to 7.14 g·Pa^{-1}·s^{-1}·m^{-1}·10^{-7} when P5-160 content was over 30%, in agreement with a previous study on pectins films (Almasi et al., 2020). The results confirmed the expected increase on water resistance when blending CH and pectins for films preparation, due to the positive interactions between the different polysaccharide components that hinder water binding and mobility. In addition, there are reports that the addition of phenolic compounds in pectin matrices improve the matrix organization and obstruct the passage of water vapor through the film (Eça, Machado, Hubinger, & Menegalli, 2015). In the present study, the high amount of ferulic acid (FA) and sinapic acid (SA) present in the P5-160 fraction (Table S3) contributed significantly to this phenomenon, since the higher amount of P5-160 in the films and, therefore, the higher presence of FA and SA, the lower WVP.

The influence of P5-160 incorporation on mechanical properties of CH-based films is shown in Table 1 and Fig. 3d. As shown, the addition of 10% P5-160 increased the stress at break of the films (31.64 MPa for 90:10 CH:P and 20.85 MPa for 100% CH). When the amount of P5-160 was increased to 20%, even though it presented similar resistance (21.91 MPa), the film material was more rigid presenting a lower percentage strain (1.31% for 80:20 CH:P in comparison with 1.61% for 100% CH). Thereafter, the addition of higher amounts of BTPW carbohydrates resulted in a deterioration of both stress (11.66 MPa and 2.78 MPa for 70:30 CH:P and 60:40 CH:P, respectively) and percentage strain (1.09% and 0.55% for 70:30 CH:P and 60:40 CH:P). However, the improved mechanical properties with 10% of P5-160 in the film were reflected in the Young's Modulus, 2901.2 MPa compared with 2590.5 MPa of 100% CH film (Table 1).

In the present study, it seems that at low BTPW-P concentrations (10 and 20%), films show improved their properties due to the good compatibility between CH and BTPW-P (as reported for the density values). However, the mechanical properties of the films worsened at higher P5-160 concentrations because of the lower dispersion of the BTPW carbohydrates in the mix with CH, which prevented the films from forming properly, making them weaker to tensile strength.

In short, increasing the amount of P5-160 in CH films improved water barrier properties but decreased the mechanical strength. According to Rashidova et al. (2004), the CH-pectin complex is formed at the expense of electrostatic interaction between the positively charged amino groups on the C-2 pyranose ring of CH and the negatively charged carboxyl groups on the C-5 pyranose ring of P5-160 fraction (Fig. 4).

Regardless of the initial ratio of the matrix components, the formation of the CH-P complex occurs in stoichiometric proportions. For CH:P ratios other than 1:1, the structural toughness of the suspension is determined by the P-fraction content. Thus, these authors confirmed that a higher P-fraction content resulted in a higher gel toughness (e.g.,

Table 1
Physical (density, WVTR[a], WVP[b]), mechanical (tensile strength, Young's modulus, stress at break, strain) and optical (transparency, UV-light barrier) properties of chitosan:pectins (CH:P) hybrid films.

Film sample	Density (g/cm^3)	WVTR (g·m^{-2}·h^{-1})	WVP (g·Pa^{-1}·s^{-1}·m^{-1}·10^{-7})	Tensile strength (MPa)	Young's modulus (MPa)	Stress at break (MPa)	Strain (%)	Transparency (%)	UV-light barrier (%)
100% CH	0.91 ± 0.01	53.21 ± 4.90	17.76 ± 2.34	23.11 ± 0.64	2590.5 ± 21.35	20.85 ± 0.61	1.61 ± 0.12	52.17	55.26
90:10 CH:P	1.03 ± 0.04	36.13 ± 0.49	14.53 ± 0.20	31.31 ± 1.11	2901.2 ± 186.32	31.64 ± 2.69	1.68 ± 014	51.31	95.53
80:20 CH:P	1.09 ± 0.04	25.10 ± 2.54	10.59 ± 1.07	16.07 ± 3.96	1483.9 ± 60.10	21.91 ± 1.87	1.31 ± 0.20	48.60	99.57
70:30 CH:P	0.98 ± 0.06	20.00 ± 1.10	7.14 ± 0.39	11.38 ± 1.91	1310.5 ± 78.57	11.66 ± 0.40	1.09 ± 0.01	45.58	99.62
60:40 CH:P	0.84 ± 0.02	27.01 ± 3.30	7.13 ± 1.69	5.76 ± 0.78	1286.2 ± 103.79	2.78 ± 0.07	0.55 ± 0.06	45.27	99.98

[a] WVTR: water vapor transmission rate.
[b] WVP: water vapor permeability.

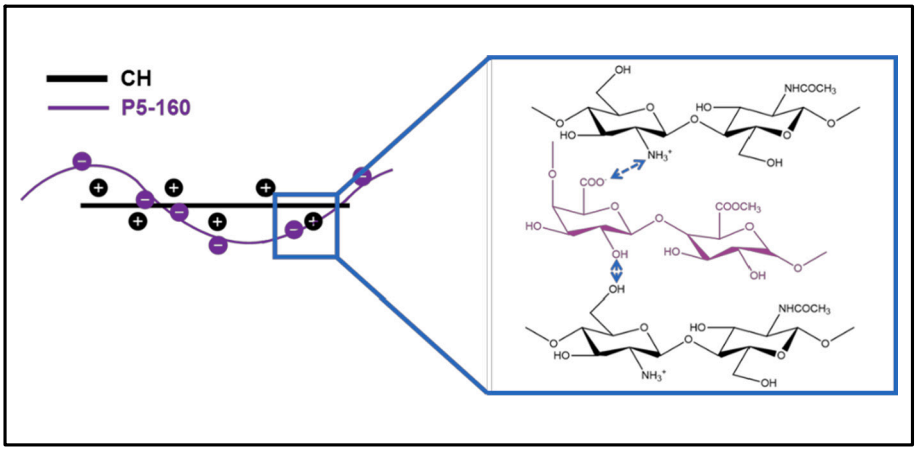

Fig. 4. Electrostatic interaction between CH and P5-160 fraction.

for a 3:7 CH:P ratio the toughness was significantly higher than for a 7:3 ratio). Comparing these results with the present study, the toughness of the suspensions would significantly increase in the case of 70:30 CH:P and 60:40 CH:P films. Interestingly, these same films showed the maximum improvement on water vapor barrier properties. It seems that incorporation of 30 and 40% P-fraction in CH films led to a partial collapse of the gel network significantly decreasing WVP (Hoagland & Parris, 1996). The decrease in the mechanical strength with increasing P-fraction content may be attributed to this same collapse of the structure due to the difference in the degrees in CH protonation ($-NH_3^+$) and P5-160 deprotonation ($-COO^-$) under film formation. At higher P5-160 concentration, CH molecules are more intensively charged than P5-160 molecules, meaning that the system provides more P5-160 molecules than CH counterparts (Younis & Zhao, 2019).

3.5. Transparency and UV-blocking of films

Optical properties (transparency and UV-light barrier capacity) of the prepared films, obtained from the transmittance scan in the UV–Vis region (Fig. S2), are displayed in Table 1. The color of the film was also darker while adding more concentration of P5-160 fraction, due to natural color of the carbohydrate extracted by SWE (Fig. 3a). Transparency slightly decreased when P5-160 fraction was added to the CH matrix, from 52.17% transparency for 100% CH film to 45.27% transparency for 60:40 CH:P film. The presence of P5-160 carbohydrates can cause reflection and dispersion of the incident light at the two-phase interface, thus giving rise to a high opacity in the hybrid films (Younis & Zhao, 2019). Moreover, as previously mentioned, as the amount of P5-160 increases, the structure of the matrix decreases the separation between the polymer chains due to the increase of double bonds and cyclic structures of the phenolic compounds. This causes less and less light to pass through the film, increasing the opacity (Bierhalz, da Silva, & Kieckbusch, 2012; Eça et al., 2015).

Regarding the UV-light barrier capacity all the films containing P5-160 carbohydrates almost reached 100% UV-blocking, in contrast to the CH film, which did not reach 60% (Table 1). Some authors have reported that the presence of pectins in films increases UV-light absorption due to the presence of double bonds and the cyclic structures of phenolic compounds (Eça et al., 2015; Li, Miao, Wu, Chen, & Zhang, 2014). The phenolic acid-rich profile of the P5-160 fraction (Table S3) seems to contribute favorably to this increased UV-light absorption as the amount of P5-160 in the films increases. This excellent improvement in UV-blocking capacity is a beneficial factor to evaluate the application of the films in the food packaging industry. UV-light is one of the most common initiators of degradation in food since produces lipid oxidation (Rincon et al., 2019).

3.6. Radical scavenging performance

The radical scavenging activity of pure CH and P5-160 fraction was evaluated in terms of their EC_{50} values. Pure CH did not show any antioxidant activity, while P5-160 fraction exhibited an EC_{50} value of 3 mg/mg DPPH, showing a great antioxidant performance compare with standards (ferulic and ascorbic acids, Fig. S3). This high EC_{50} for P5-160 fraction can be ascribed to the high amount of phenolic acids present in the fraction (Fig. 2b) (Butsat, Weerapreeyakul, & Siriamornpun, 2009; Rivas, Conde, Moure, Domínguez, & Parajó, 2013). DPPH radical scavenging abilities on film samples were studied in three cycles (steps). As illustrated in Fig. 5a, the CH film showed poor capacity for scavenging the DPPH radical, a result consistent with that reported in literature (Tan et al., 2019).

The incorporation of P5-160 fraction in the CH matrix rendered a radical scavenging activity higher than 95% in all concentrations tested in Step 1 (Table S4). In the second addition step of oxidant radical it could be stated that the activity was maintained equally, regardless of the percentage of P5-160 fraction present in the film. It was not until the third addition step when the 90:10 film showed a decreased scavenging capacity, 56.65% of the total radical has been scavenged. For the 80:20 film the same trend is observed maintaining still 83.80% of the scavenging activity in that case. From then on, higher amounts of P5-160 fraction maintained a complete radical activity, so the antioxidant performance was maximal within the 3-addition step of the oxidative agent. This suggests that the total amount of pectins necessary to remove the radical agent in the third step (0.35 mg DPPH) is found only in films containing more than 30% pectins in their composition.

Similar results have been reported by other authors with high radical scavenging activity by DPPH (95.42%–96.25%) in films formed by CH, pectins and tea polyphenols (Gao et al., 2019). However, their strong activity was attributed to the addition of tea polyphenols since the control films (consisting of CH and pectins) exhibited low radical scavenging activity (19%). Therefore, it seems that the high content of attached phenolic acids present in P5-160 fraction was sufficient to reach the maximum radical activity, without the need to add extra polyphenols. It has been previously reported that the presence of phenolic acids linked to polysaccharides gives them the ability to present high antioxidant capacity (Zhang, Xiao, Chen, Wei, & Liu, 2020). This fact is very desirable if these polymers are used in food preservation.

3.7. Antibacterial activity

Prior to the study of the antibacterial activity of the films, the MIC of the CH used as matrix was studied. The MIC obtained were 100 μg/mL,

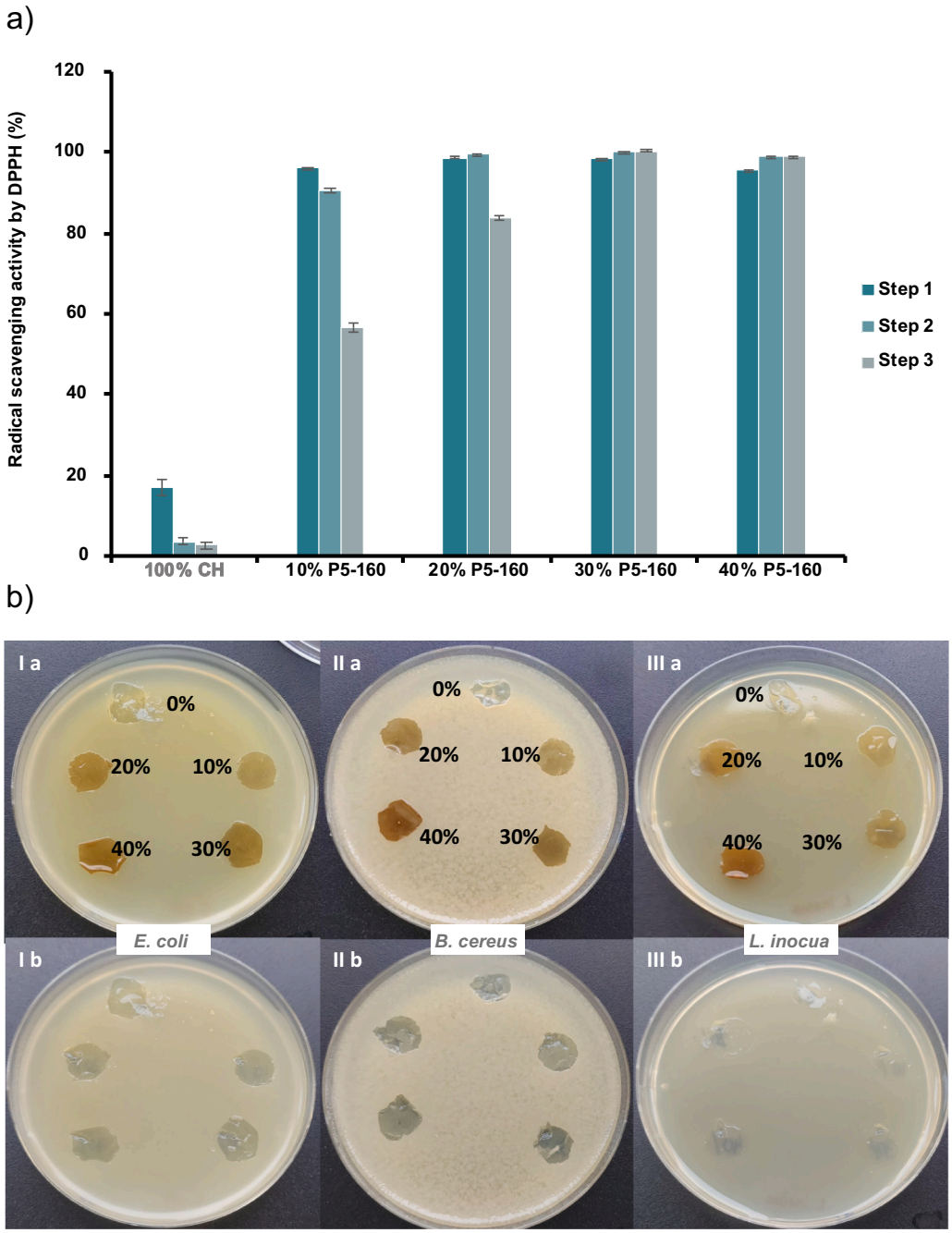

Fig. 5. a) Radical scavenging activity in chitosan:pectins (CH:P) hybrid films, and b) photographs of the antibacterial activity of film samples against *E. coli* (Ia, back plate; Ib, plate without films), *B. cereus* (IIa, back plate; IIb, plate without films), and L. *innocua* (IIIa, back plate; IIIb, plate without films).

100 μg/mL, and 500 μg/mL for *E. coli*, *B. cereus*, and *L. innocua*, respectively. These results were consistent with previous studies where the MIC of CH for *E. coli* was 80–100 μg/mL (Shanmugam, Kathiresan, & Nayak, 2016), for *B. cereus* was 62.5–125 μg/mL (Tamara, Lin, Mi, & Ho, 2018) and for *L. innocua* was 300–600 μg/mL, where the poorer antimicrobial effect of the chitosan was explained by the low negative charges of the cell compare to *E. coli* (Jung & Zhao, 2013). The low negative charges on the cell wall of *L. innocua* prevent the interaction with the cationic amino groups of chitosan which can explain the results obtained with a %-fold higher MIC for this bacteria. These microorganisms are pathogen that poses a health challenge, causing various intestinal diseases and can be present in food systems. Therefore, when developing new food packaging, it is important to consider the use of compounds with the capacity to inhibit microorganism growth (Granum & Lindbäck, 2012).

The antimicrobial activity of the film samples, studied by the agar diffusion method, is shown in Fig. 5b. The growth of the microorganisms studied was inhibited by direct contact with the films, however not diffusive inhibition halo was observed around them.

This inhibition was totally independent of the concentration of P5-160 fraction present in the films. Therefore, it could be stated that the antimicrobial activity of CH was maintained due to its positively charged amino groups. These charges interact with the negative charge of the microbial membranes causing them to disrupt and release proteins and other intracellular constituents. Very similar results were reported previously in the literature for CH, glucomannan, and nisin blend-films (Li et al., 2006). In this study the authors attributed the fully antimicrobial capacity of the films to chitosan molecules.

4. Conclusions

Polymeric carbohydrates from bay tree pruning waste (BTPW) were isolated by sequential subcritical water extraction (S-SWE) at increasing temperatures (100, 120, 140 and 160 °C) for four fixed times (5, 10, 15 and 20 min). It was found that precipitated polymers obtained at S-SWE of 5 min at 160 °C (P5-160) were highly enriched in carbohydrates (676.73 mg/g) with an exceptional content in pectins preserving attached phenolic acids. Therefore, P5-160 fraction was used for the preparation of hybrid chitosan films. Films containing 10% of P5-160 fraction considerably improved the tensile strength and elastic modulus. Films containing 20% of P5-160 showed a higher density (1.03 g/cm^3) as well as a very desirable water vapor permeability in food packaging systems (10.59 g·Pa^{-1}·s^{-1}·m^{-1}·10^{-7}). The optical properties and antioxidant capacity were not significantly different between 10 or 20% of BTPW carbohydrates in the chitosan matrix, which did improve considerably in both cases. Hybrid films from chitosan and BTPW carbohydrates are suitable for application in food active packaging. Due to their antimicrobial capacity regardless the concentration of BTPW carbohydrates added, indicating that the antimicrobial activity of the chitosan was correctly maintained in all cases.

Supplementary data to this article can be found online at https://doi.org/10.1016/j.carbpol.2021.118477.

CRediT authorship contribution statement

E. Rincón: Conceptualization, Methodology, Formal analysis, Investigation, Writing – original draft, Writing – review & editing, Visualization. **E. Espinosa:** Conceptualization, Investigation, Writing – original draft, Writing – review & editing. **M.T. García-Domínguez:** Methodology, Formal analysis. **A.M. Balu:** Writing – review & editing, Supervision. **F. Vilaplana:** Resources, Writing – original draft, Writing – review & editing, Funding acquisition. **L. Serrano:** Resources, Writing – review & editing, Funding acquisition, Supervision. **A. Jiménez-Quero:** Conceptualization, Methodology, Investigation, Visualization, Writing – original draft, Writing – review & editing, Supervision, Project administration.

Acknowledgements

Authors would like to thank the Spanish Ministry of Science and Innovation (Ramon y Cajal contract RYC-2015-17109) and Universidad de Córdoba, Spain (Predoctoral Grant 2019) for the financial support during this work.

References

Almasi, H., Azizi, S., & Amjadi, S. (2020). Development and characterization of pectin films activated by nanoemulsion and Pickering emulsion stabilized marjoram (*Origanum majorana* L.) essential oil. *Food Hydrocolloids, 99*, Article 105338.

Azeredo, A. M. C., Morrugares-Carmona, R., Wellner, N., Cross, K., Bajka, B., & Waldron, K. W. (2016). Development of pectin films with pomegranate juice and citric acid. *Food Chemistry, 198*, 101–106.

Bierhalz, A. C. K., da Silva, M. A., & Kieckbusch, T. G. (2012). Natamycin release from alginate/pectin films for food packaging applications. *Journal of Food Engineering, 110*(1), 18–25.

Brand-Williams, W., Cuvelier, M. E., & Berset, C. (1995). Use of a free radical method to evaluate antioxidant activity. *LWT - Food Science and Technology, 28*(1), 25–30.

Butsat, S., Weerapreeyakul, N., & Siriamornpun, S. (2009). Changes in phenolic acids and antioxidant activity in Thai rice husk at five growth stages during grain development. *Journal of Agricultural and Food Chemistry, 57*(11), 4566–4571.

Casado Muñoz, M. C., Benomar, N., Lerma, L. L., Gálvez, A., & Abriouel, H. (2014). Antibiotic resistance of *Lactobacillus pentosus* and *Leuconostoc pseudomesenteroides* isolated from naturally-fermented Aloreña table olives throughout fermentation process. *International Journal of Food Microbiology, 172*, 110–118.

Chen, J., Cheng, H., Zhi, Z., Zhang, H., Linhardt, R. J., Zhang, F., & Ye, X. (2021). Extraction temperature is a decisive factor for the properties of pectin. *Food Hydrocolloids, 112*, Article 106160.

Coetzee, B., Schols, H. A., & Wolfaardt, F. (2011). Determination of pectin content of eucalyptus wood. *Holzforschung, 65*(3), 327–331.

Costa, M. J., Cerqueira, M. A., Ruiz, H. A., Fougnies, C., Richel, A., Vicente, A. A., & Aguedo, M. (2015). Use of wheat bran arabinoxylans in chitosan-based films: Effect on physicochemical properties. *Industrial Crops and Products, 66*, 305–311.

De Farias Silva, C. E., & Bertucco, A. (2018). Severity factor as an efficient control parameter to predict biomass solubilization and saccharification during acidic hydrolysis of microalgal biomass. *BioEnergy Resources, 11*, 491–504.

Eça, K. S., Machado, M. T. C., Hubinger, M. D., & Menegalli, F. C. (2015). Development of active films from pectin and fruit extracts: Light protection, antioxidant capacity, and compounds stability. *Journal of Food Science, 80*(11), 2389–2396.

FAO. (2019). Food and agriculture data (FAOSTAT). http://www.fao.org/faostat/en/#data Accessed: 25/02/2021.

Gao, H. X., He, Z., Sun, Q., He, Q., & Zeng, W. C. (2019). A functional polysaccharide film forming by pectin, chitosan, and tea polyphenols. *Carbohydrate Polymers, 215*, 1–7.

Granum, P. E., & Lindbäck, T. (2012). Bacillus cereus. In M. P. Doyle, & R. L. Buchanan (Eds.), *Food microbiology*. Wiley.

Hoagland, P. D., & Parris, N. (1996). Chitosan/pectin laminated films. *Journal of Agricultural and Food Chemistry, 44*(7), 1915–1919.

International, A. (2010). *ASTM E96/E96M-10, standard test methods for water vapor transmission of materials*. West Conshohocken, PA.

International, A. (2018). *ASTM D882-18, standard test method for tensile propertes of thin plastic sheetings*. West Conshohocken, PA.

Jin, X., Hu, Z., Wu, S., Song, T., Yue, F., & Xiang, Z. (2019). Promoting the material properties of xylan-type hemicelluloses from the extraction step. *Carbohydrate Polymers, 215*, 235–245.

Jung, J., & Zhao, Y. (2013). Impact of the structural differences between α- and β-chitosan on their depolymerizing reaction and antibacterial activity. *Journal of Agricultural and Food Chemistry, 61*(37), 8783–8789.

Lachos-Perez, D., Baseggio, A. M., Torres-Mayanga, P. C., Ávila, P. F., Tompsett, G. A., Marostica, M., & Forster-Carneiro, T. (2020). Sequential subcritical water process applied to orange peel for the recovery flavanones and sugars. *The Journal of Supercritical Fluids, 160*, Article 104789.

Lazaridou, A., & Biliaderis, C. G. (2020). Edible films and coatings with pectin. In V. Kontogiorgos (Ed.), *Pectin: Technological and physiological properties* (pp. 99–123). Cham: Springer International Publishing.

Le Normand, M., Edlund, U., Holmbom, B., & Ek, M. (2012). Hot-water extraction and characterization of spruce bark non-cellulosic polysaccharides. *Nordic Pulp and Paper Research Journal, 27*, 18–23.

Li, B., Kennedy, J. F., Peng, J. L., Yie, X., & Xie, B. J. (2006). Preparation and performance evaluation of glucomannan–chitosan–nisin ternary antimicrobial blend film. *Carbohydrate Polymers, 65*(4), 488–494.

Li, J. H., Miao, J., Wu, J. L., Chen, S. F., & Zhang, Q. Q. (2014). Preparation and characterization of active gelatin-based films incorporated with natural antioxidants. *Food Hydrocolloids, 37*, 166–173.

Maciel, V. B. V., Yoshida, C. M. P., & Franco, T. T. (2015). Chitosan/pectin polyelectrolyte complex as a pH indicator. *Carbohydrate Polymers, 132*, 537–545.

Mao, G., Wu, D., Wei, C., Tao, W., Ye, X., Linhardt, R. J., & Chen, S. (2019). Reconsidering conventional and innovative methods for pectin extraction from fruit and vegetable waste: Targeting rhamnogalacturonan I. *Trends in Food Science & Technology, 94*, 65–78.

Marić, M., Grassino, A. N., Zhu, Z., Barba, F. J., Brnčić, M., & Rimac Brnčić, S. (2018). An overview of the traditional and innovative approaches for pectin extraction from plant food wastes and by-products: Ultrasound-, microwaves-, and enzyme-assisted extraction. *Trends in Food Science & Technology, 76*, 28–37.

Mathew, S., & Abraham, T. E. (2008). Characterisation of ferulic acid incorporated starch–chitosan blend films. *Food Hydrocolloids, 22*(5), 826–835.

Maxwell, E. G., Belshaw, N. J., Waldron, K. W., & Morris, V. J. (2012). Pectin — An emerging new bioactive food polysaccharide. *Trends in Food Science & Technology, 24*(2), 64–73.

McKee, L. S., Sunner, H., Anasontzis, G. E., Toriz, G., Gatenholm, P., Bulone, V., & Olsson, L. (2016). A GH115 α-glucuronidase from *Schizophyllum commune* contributes to the synergistic enzymatic deconstruction of softwood glucuronoarabinoxylan. *Biotechnology for Biofuels, 9*(1), 2.

Menzel, C., González-Martínez, C., Chiralt, A., & Vilaplana, F. (2019). Antioxidant starch films containing sunflower hull extracts. *Carbohydrate Polymers, 214*, 142–151.

Norcino, L. B., de Oliveira, J. E., Moreira, F. K. V., Marconcini, J. M., & Mattoso, L. H. C. (2018). Rheological and thermo-mechanical evaluation of bio-based chitosan/pectin blends with tunable ionic cross-linking. *International Journal of Biological Macromolecules, 118*, 1817–1823.

Otoni, C. G., de Moura, M. R., Aouada, F. A., Camilloto, G. P., Cruz, R. S., Lorevice, M. V., Soares, N. F. F., & Mattoso, L. H. C. (2014). Antimicrobial and physical-mechanical properties of pectin/papaya puree/cinnamaldehyde nanoemulsion edible composite films. *Food Hydrocolloids, 41*, 188–194.

Pasandide, B., Khodaiyan, F., Mousavi, Z. E., & Hosseini, S. S. (2017). Optimization of aqueous pectin extraction from *Citrus medica* peel. *Carbohydrate Polymers, 178*, 27–33.

Pedras, B. M., Regalin, G., Sá-Nogueira, I., Simões, P., Paiva, A., & Barreiros, S. (2020). Fractionation of red wine grape pomace by subcritical water extraction/hydrolysis. *The Journal of Supercritical Fluids, 160*, Article 104793.

Petkowicz, C. L. O., Vriesmann, L. C., & Williams, P. A. (2017). Pectins from food waste: Extraction, characterization and properties of watermelon rind pectin. *Food Hydrocolloids, 65*, 57–67.

Rashidova, S. S., Milusheva, R. Y., Semenova, L. N., Mukhamedjanova, M. Y., Voropaeva, N. L., Vasilyeva, S., Faizieva, R., & Ruban, I. N. (2004). Characteristics of interactions in the pectin-chitosan system. *Chromatographia, 59*, 779–782.

Ren, L., Yan, X., Zhou, J., Tong, J., & Su, X. (2017). Influence of chitosan concentration on mechanical and barrier properties of corn starch/chitosan films. *International Journal of Biological Macromolecules, 105*(3), 1636–1643.

Requena, R., Jiménez-Quero, A., Vargas, M., Moriana, R., Chiralt, A., & Vilaplana, F. (2019). Integral fractionation of rice husks into bioactive arabinoxylans, cellulose nanocrystals, and silica particles. *ACS Sustainable Chemistry & Engineering, 7*(6), 6275–6286.

Rincón, E., Balu, A. M., Luque, R., & Serrano, L. (2019). Mechanochemical extraction of antioxidant phenolic compounds from Mediterranean and medicinal *Laurus nobilis*: A comparative study with other traditional and green novel techniques. *Industrial Crops and Products, 141*, Article 111805.

Rincon, E., Serrano, L., Balu, A. M., Aguilar, J. J., Luque, R., & Garcia, A. (2019). Effect of bay leaves essential oil concentration on the properties of biodegradable carboxymethyl cellulose-based edible films. *Materials (Basel), 12*(15).

Rincón, E., Zuliani, A., Jiménez-Quero, A., Vilaplana, F., Luque, R., Serrano, L., & Balu, A. M. (2020). Combined extraction/purification-catalytic microwave-assisted conversion of *Laurus nobilis* L. pruning waste polysaccharides into methyl levulinate. *ACS Sustainable Chemistry & Engineering, 8*(29), 11016–11023.

Rivas, S., Conde, E., Moure, A., Domínguez, H., & Parajó, J. C. (2013). Characterization, refining and antioxidant activity of saccharides derived from hemicelluloses of wood and rice husks. *Food Chemistry, 141*(1), 495–502.

Rombouts, F. M., & Thibault, J. F. (1986). Feruloylated pectic substances from sugar-beet pulp. *Carbohydrate Research, 154*(1), 177–187.

Rudjito, R. C., Ruthes, A. C., Jiménez-Quero, A., & Vilaplana, F. (2019). Feruloylated arabinoxylans from wheat bran: Optimization of extraction process and validation at pilot scale. *ACS Sustainable Chemistry & Engineering, 7*(15), 13167–13177.

Ruiz, H. A., Cerqueira, M. A., Silva, H. D., Rodríguez-Jasso, R. M., Vicente, A. A., & Teixeira, J. A. (2013). Biorefinery valorization of autohydrolysis wheat straw hemicellulose to be applied in a polymer-blend film. *Carbohydrate Polymers, 92*(2), 2154–2162.

Rumpunen, K., Thomas, M., Badilas, N., & Thibault, J. F. (2002). Validation of a combined enzymatic and HPLC method for screening of pectins in fruits of Japanese quince (*Chaenomeles japonica*). *LWT - Food Science and Technology, 35*(6), 490–496.

Ruthes, A. C., Martínez-Abad, A., Tan, H. T., Bulone, V., & Vilaplana, F. (2017). Sequential fractionation of feruloylated hemicelluloses and oligosaccharides from wheat bran using subcritical water and xylanolytic enzymes. *Green Chemistry, 19*(8), 1919–1931.

Ruthes, A. C., Rudjito, R. C., Rencoret, J., Gutiérrez, A., del Río, J. C., Jiménez-Quero, A., & Vilaplana, F. (2020). Comparative recalcitrance and extractability of cell wall polysaccharides from cereal (wheat, rye, and barley) brans using subcritical water. *ACS Sustainable Chemistry & Engineering, 8*(18), 7192–7204.

Santos, E. E., Amaro, R. C., Bustamante, C. C. C., Guerra, M. H. A., Soares, L. C., & Froes, R. E. S. (2020). Extraction of pectin from agroindustrial residue with an ecofriendly solvent: Use of FTIR and chemometrics to differentiate pectins according to degree of methyl esterification. *Food Hydrocolloids, 107*, Article 105921.

Shanmugam, A., Kathiresan, K., & Nayak, L. (2016). Preparation, characterization and antibacterial activity of chitosan and phosphorylated chitosan from cuttlebone of *Sepia kobiensis* (Hoyle, 1885). *Biotechnology Reports, 9*, 25–30.

Tamara, F. R., Lin, C., Mi, F. L., & Ho, Y. C. (2018). Antibacterial effects of chitosan/cationic peptide nanoparticles. *Nanomaterials, 8*(2), 88–103.

Tan, W., Dong, F., Zhang, J., Zhao, X., Li, Q., & Guo, Z. (2019). Physical and antioxidant properties of edible chitosan ascorbate films. *Journal of Agricultural and Food Chemistry, 67*(9), 2530–2539.

Technical Association of the Pulp and Paper Industry (TAPPI). (2018). TAPPI standards: Regulation and style guidelines. Revised January. Available online: https://www.tappi.org/content/pdf/standards/tm_guidelines_complete.pdf (accesed on 29 April 2021).

Wandee, Y., Uttapap, D., & Mischnick, P. (2019). Yield and structural composition of pomelo peel pectins extracted under acidic and alkaline conditions. *Food Hydrocolloids, 87*, 237–244.

Xu, J., Xia, R., Yuan, T., & Sun, R. (2019). Use of xylooligosaccharides (XOS) in hemicelluloses/chitosan-based films reinforced by cellulose nanofiber: Effect on physicochemical properties. *Food Chemistry, 298*, Article 125041.

Xu, J., Xia, R., Zheng, L., Yuan, T., & Sun, R. (2019). Plasticized hemicelluloses/chitosan-based edible films reinforced by cellulose nanofiber with enhanced mechanical properties. *Carbohydrate Polymers, 224*, Article 115164.

Xu, Y. X., Kim, K. M., Hanna, M. A., & Nag, D. (2005). Chitosan–starch composite film: Preparation and characterization. *Industrial Crops and Products, 21*(2), 185–192.

Yang, J. S., Mu, T. H., & Ma, M.-M. (2018). Extraction, structure, and emulsifying properties of pectin from potato pulp. *Food Chemistry, 244*, 197–205.

Younis, H. G. R., Abdellatif, H. R. S., Ye, F., & Zhao, G. (2020). Tuning the physicochemical properties of apple pectin films by incorporating chitosan/pectin fiber. *International Journal of Biological Macromolecules, 159*, 213–221.

Younis, H. G. R., & Zhao, G. (2019). Physicochemical properties of the edible films from the blends of high methoxyl apple pectin and chitosan. *International Journal of Biological Macromolecules, 131*, 1057–1066.

Zhang, H., Chen, J., Li, J., Yan, L., Li, S., Ye, X., & Chen, S. (2018). Extraction and characterization of RG-I enriched pectic polysaccharides from mandarin citrus peel. *Food Hydrocolloids, 79*, 579–586.

Zhang, X., Wei, Y., Chen, M., Xiao, N., Zhang, J., & Liu, C. (2020). Development of functional chitosan-based composite films incorporated with hemicelluloses: Effect on physicochemical properties. *Carbohydrate Polymers, 246*, Article 116489.

Zhang, X., Xiao, N., Chen, M., Wei, Y., & Liu, C. (2020). Functional packaging films originating from hemicelluloses laurate by direct transesterification in ionic liquid. *Carbohydrate Polymers, 229*, Article 115336.

Zou, Y., Zhang, B. Z., Barsett, H., Inngjerdingen, K., Diallo, D., Michaelsen, T., & Paulsen, B. (2014). Complement fixing polysaccharides from *Terminalia macroptera* root bark, stem bark and leaves. *Molecules, 19*, 7440–7458.